Fabrication of chemically and structurally abrupt $Eu_{1-x}La_xO$/SrO/Si interfaces and their analysis by STEM-EELS

R. Held,[1] J. A. Mundy,[2] M. E. Holtz,[2] D. Hodash,[1] T. Mairoser,[3] D. A. Muller,[2,4] and D. G. Schlom [1,4,5]

[1]*Department of Materials Science and Engineering, Cornell University, Ithaca, New York 14853, USA*
[2]*School of Applied and Engineering Physics, Cornell University, Ithaca, New York 14853, USA*
[3]*Zentrum für Elektronische Korrelationen und Magnetismus, Universität Augsburg, Universitätsstraße 1, D-86159 Augsburg, Germany*
[4]*Kavli Institute at Cornell for Nanoscale Science, Ithaca, New York 14853, USA*
[5]*Leibniz-Institut für Kristallzüchtung, Max-Born-Straße 2, 12489 Berlin, Germany*

Precise control of molecular-beam epitaxy deposition conditions has enabled the fabrication of chemically and structurally abrupt $Eu_{1-x}La_xO$/SrO/Si interfaces by interposing as little as half a monolayer of SrO between the La-doped EuO and silicon. The interfaces were analyzed by scanning transmission electron microscopy-electron energy loss spectroscopy; no reaction products were detected. These abrupt interfaces might enable direct ohmic injection of spin-polarized currents from the doped half-metallic semiconductor EuO into silicon.

I. INTRODUCTION

Some of the most important goals of spintronics, such as the fabrication of spin transistors and their implementation into mainstream semiconductor technology, rely on the successful injection of spin-polarized currents into the host semiconductor. Unfortunately, injection from metallic ferromagnetic electrodes such as cobalt and NiFe alloys is hindered by the incomplete spin polarization of these materials and a fundamental obstacle known as the conductivity mismatch problem [1]. This problem, caused by the differing conductivities of the injector and host materials, dramatically reduces the spin injection efficiency. To achieve spin injection this effect has to be circumvented, which is typically done by using highly resistive tunnel or Schottky barriers between a ferromagnet and the host semiconductor [2–34].

Spin injection from highly spinpolarized materials that exhibit effective electrical resistances close to the effective resistance of the host semiconductor provides an alternative approach for studying spin injection effects and may ultimately lead to higher spin injection efficiencies. This strategy is known as direct ohmic spin injection [5]. Unfortunately, semiconducting materials with high spin polarizations and tunable effective resistances that can be deposited directly on semiconductors are extremely rare. Therefore, experimental ohmic spin injection research is still in its infancy.

The $\geqslant 90\%$ spin polarization of charge carriers in La-doped EuO [6] and 96% spin polarization in Lu-doped EuO [7] demonstrated by Andreev reflection measurements, combined with the ability to grow EuO epitaxially on silicon [6], GaN [6], and GaAs [8], make doped EuO an excellent candidate material for ohmic injection of spin-polarized currents directly into these mainstream semiconductors. The mechanism leading to the half metallicity of EuO is the 0.6-eV exchange splitting of the conduction band [9] below the Curie

temperature, T_C. For ohmic spin injection it is important that EuO is not only a half-metallic ferromagnet, but also that it is semiconducting. By doping EuO with trivalent rare earth ions such as gadolinium, lanthanum, and lutetium, the conductivity of EuO can be tuned by orders of magnitude to precisely match the conductivity of the host semiconductor [6,10–14]. Importantly, doping EuO has been shown to have a negligible effect on its high spin polarization [6,7].

Stoichiometric EuO has a Curie temperature T_C of 69 K [15], well below the T_C needed for commercial devices. Nevertheless, the unique combination of properties renders EuO an outstanding material for proof-of-concept spintronic devices and fundamental spintronic studies, which are needed for a better understanding of the experimental difficulties and the potential of ohmic spin injection. Furthermore, by doping with oxygen vacancies or rare earth ions, the T_C of EuO can be increased up to about 130 K [10–14,16–20] and compressive strain is expected to further enhance T_C [21,22].

Deposition of single-crystalline EuO thin films on silicon substrates by molecular-beam epitaxy (MBE) has been demonstrated with and without using SrO buffer layers, but no spin signals have been reported yet [6,23–31]. Unfortunately, even thin interfacial impurity layers are expected to interfere with efficient spin injection [32]. This is because the formation of europium silicides and compounds with higher europium oxidation states are expected to change the magnetic properties of the interface. This could dramatically reduce the spin injection efficiency, e.g., by spin-flip scattering. In addition, unwanted phases could alter the electrical resistance of the interface and therefore interfere with conductance matching between film and substrate. Atomically clean interfaces without unwanted phases are therefore expected to be a fundamental requirement for achieving high spin injection efficiencies.

Extensive work has been done on the optimization of EuO/Si deposition procedures with the goal of reducing the

amount of reaction products at the interface and the optimization of the structural perfection of the EuO films. In one approach, Caspers *et al.* used an *in situ* hydrogen passivation of (001) Si followed by oxygen-protective europium monolayers to deposit EuO directly on silicon [24,28]. Sample characterization by hard x-ray photoemission spectroscopy (HAXPES) resulted in a mean europium silicide thickness of $\sim$0.14 nm and an EuO/Si interface oxidation minimum value of $\sim$0.697 nm [28]. The abruptness of the resulting interface was characterized by high-resolution transmission electron microscopy (HR-TEM) [28].

In another approach, Averyanov *et al.* deposited EuO directly on (001) Si without using any buffer layers [26,27]. They used *in situ* reflection high-energy electron diffraction (RHEED), Rutherford backscattering spectrometry (RBS), and, after deposition of capping layers, *ex situ* x-ray diffraction (XRD) and superconducting quantum interference device (SQUID) measurements to develop a deposition procedure that yielded EuO films with no signs of unwanted phases or off stoichiometry according to these measurements.

In a subsequent study, Averyanov *et al.* used a modified deposition procedure to deposit EuO films on (111) Si [30]. The resulting (111) EuO films showed a $\sim$5 EuO monolayer (ML) or $\sim$1.3-nm-thick disordered interface layer in high-angle annular dark-field scanning transmission electron microscopy (HAADF-STEM) images. X-ray diffraction (XRD) scans and SQUID measurements showed no signs of unwanted phases.

Most recently, Averyanov *et al.* investigated the atomic interface structure of EuO/Si films deposited at a substrate temperature T_{Sub} of just 100 °C using HAADF-STEM [31]. These experiments featured europium metal coverages of the pristine Si surface corresponding to 1/2, 3/5, and 2/3 ML before starting EuO deposition, that all led to different surface reconstructions initially. After deposition of 6 nm of EuO, the interfaces of all samples looked the same in HAADF-STEM measurements and also showed very similar structural properties according to XRD and the same saturation magnetic moments and Curie temperatures. The authors pointed out that the samples may still exhibit different atomic microstructures when the presence and position of oxygen atoms in the interface are also taken into account (oxygen atoms are not visible in the HAADF-STEM images). This could in principle be inferred from the distance between the first oxide and the topmost silicon layers. This distance was, however, inconclusive for the EuO/Si(001) interfaces, i.e., it is very difficult to determine the valence states of the atoms at the EuO/Si interface from atomic positions measured by HAADF-STEM.

Mundy *et al.* characterized EuO films grown on (001) Si by STEM-EELS that measures the europium valence states at the same time that it provides structural characterization of the interface with atomic resolution [25]. EuO films grown directly on silicon were observed to have disordered layers at the interfaces. But more importantly, these measurements also revealed the presence of a europium silicide reaction product in a $\sim$2-nm-thick layer, including $EuSi_2$ and europium ions exhibiting 3+ valence. In these samples small additional peaks could even be seen in θ-2θ XRD measurements. Additional EuO/SrO/Si samples containing two monolayers (MLs) or 5 MLs of SrO at the interface have also been investigated [6,25]. These SrO buffer layers allowed the deposition of

EuO films with no detectable additional peaks in the θ-2θ– measurements. Nonetheless, STEM-EELS measurements of these samples revealed the presence of disordered regions and impurity phases at the interfaces even in the samples with thicker SrO buffer layers [25].

The aforementioned results demonstrate the difficulty of avoiding reaction products at the EuO/Si interface and show that characterization solely by methods like RHEED, XRD, and SQUID magnetometry can be insufficient to exclude the presence of impurity phases at the interface. The thicknesses of the reaction layer can be too small for XRD to detect and additional phases may also not be detectable by RHEED, as they could be amorphous, highly disordered, grow epitaxially and have similar lattice spacing and symmetry as the desired phase, or evolve with time and deposition and no longer be visible by RHEED as the interface to silicon becomes buried with additional growth of EuO.

HAADF-STEM is a powerful tool to investigate the atomic structure at the EuO/Si interface; however, it is very difficult to extract information on the valence states of the atoms at the interface from HAADF-STEM images. In contrast, STEM-EELS is able to detect valence changes and even very small amounts of additional phases and therefore is ideally suited to investigate EuO/Si and EuO/SrO/Si interfaces.

In this work we investigate the growth of undoped and doped EuO on silicon by MBE to identify routes to avoid the formation of impurity phases at the interface. As we expect conductance matching by doping with oxygen vacancies to be very difficult to control and because oxygen-deficient growth conditions favor the formation of europium silicides at the EuO/Si interface [25], we focus on the investigation of rare-earth-doped EuO. As a dopant we use lanthanum, as the dependence of the properties such as Curie temperature and resistivity of EuO on lanthanum doping are known quite well [14]. By employing relatively low growth temperatures and precise control of the deposition conditions we achieve EuO/SrO/Si and $Eu_{1-x}La_xO$/SrO/Si structures with clean interfaces as demonstrated by STEM-EELS measurements. For our deposition conditions, a minimum of $\frac{1}{2}$ ML of SrO is required to avoid unwanted reactions between the doped or undoped EuO and silicon.

II. METHODS

Typically, EuO thin films are grown in an adsorption-controlled regime that exploits the relatively high vapor pressure of europium metal as compared to EuO. At sufficiently high substrate temperatures, $T_{Sub} \gtrsim 375$ °C, the growth rate of EuO under europium-rich conditions is determined by $P(O_2)$; excess europium metal atoms re-evaporate from the surface of the stoichiometric EuO crystal during growth [33,34]. At these temperatures, the growth of high-quality undoped and rare-earth-doped EuO films has been demonstrated [6,11,13,14,20,22–30]. Unfortunately, higher deposition temperatures also lead to enhanced interdiffusion, which is a typical reason for the formation of unwanted phases and magnetic impurities at interfaces that can hinder spin injection from half metals into semiconductors [25]. Therefore, we

investigated the possibility of growing high-quality films at lower temperatures.

By optimizing deposition conditions we found a growth window for EuO thin films on YAlO$_3$ for temperatures down to 200 °C in which no RHEED extra spots appeared after deposition of ∼35 nm EuO and XRD showed no signs of other phases (see the Supplemental Material [35]) for further details on the optimization of the deposition method). After deposition of the EuO, the samples were cooled to T_{Sub} < 100 °C in vacuum and protected from further oxidation by deposition of a 50–100-nm-thick polycrystalline aluminum or amorphous silicon capping layer. In SQUID measurements, undoped EuO films that were deposited within the growth window exhibited T_C values of 69 ± 1 K, consistent with stoichiometric EuO [15]. Transport measurements of bridges pattered into silicon-capped samples grown on YAlO$_3$ showed high resistances, > 5 GΩ at 5 K, ruling out the presence of a significant concentration of oxygen vacancies (see Ref. [6] for a description of the patterning and *in situ* contacting procedure). Therefore, we conclude that samples grown within this growth window are very close to stoichiometric.

Using the optimized deposition conditions described, we grew epitaxial EuO films on (001)-oriented silicon substrates with and without SrO buffer layers. For the deposition of SrO buffer layers we followed a recipe similar to the one described in Ref. [25]. In brief, the process consists of thermal desorption of the native oxide of the silicon wafer at T_{Sub} ∼ 950 °C for 5 min, followed by cooling the wafer in vacuum to T_{Sub} ∼ 700 °C and depositing 1 ML or $\frac{1}{2}$ ML of strontium metal [where 1 ML is the concentration of atoms on the (001) surface of silicon, 6.78 × 10^{14} $\frac{atoms}{cm^2}$]. The amount of strontium metal required for the specific coverage was calibrated using *in situ* quartz crystal microbalance measurements that typically were accurate within a few percent. After further cooling to T_{Sub} ∼ 200 °C we stabilized $P(O_2)$ at the value used for growth (∼2.5 × 10^{-8} Torr) and initiated the EuO deposition at the designated growth temperature. For fine-tuning of the oxygen pressure we developed a RHEED-based method that exploited the occurrence of various characteristic diffraction patterns as a function of the radial position of the RHEED beam on the silicon wafer (see the Supplemental Material for more information [35]).

III. RESULTS

For ohmic spin injection, conductance-matched EuO/Si interfaces free of reaction phases and intervening buffer layers are expected to be ideal. But even with the optimized deposition conditions we were not able to grow high-quality EuO directly on silicon. When introducing oxygen into the chamber (∼2.5 × 10^{-8} Torr) prior to the EuO deposition, the deoxidized silicon wafer surface quickly oxidized again leading to the loss of epitaxy at all tested temperatures between T_{Sub} ∼ 70 °C and T_{Sub} ∼ 400 °C as detected by RHEED. Opening the europium shutter during the ramp-up of $P(O_2)$ improved epitaxy, but only if this were done at an early stage, where $P(O_2)$ had not yet reached the value found necessary for high-quality growth on YAlO$_3$. For such early opening of the europium shutter, we expect oxygen-poor growth conditions that allow epitaxy of EuO on silicon, but only at

the cost of the formation of a europium silicide layer at the interface [25].

Combining our RHEED and XRD results with the results in the literature (RHEED, XRD, HAADF-STEM, HAXPES) reporting the growth of EuO directly on silicon [6,23–31], we conclude that successful epitaxial growth of EuO *directly* on silicon typically is mediated by the formation of a europium silicide layer of varying thickness. This assumption is also consistent with previous STEM-EELS findings [25]. At $P(O_2)$ pressures high enough to avoid formation of these compounds on the bare silicon surface, the silicon surface quickly oxidizes and the perfection of the epitaxial growth suffers greatly or is not achieved, leading to partially polycrystalline or amorphous films according to RHEED. At lower pressures, or with a certain europium metal coverage of the pristine silicon surface, a europium silicide layer forms at the EuO/Si interface, which provides a suitable structural template for subsequent epitaxial growth of EuO. The presence of a thick europium silicide layer would certainly be expected to act as a barrier for the injection of spin-polarized currents. Up to now it is not clear whether the presence of a submonolayer thickness of these silicides leads to the same effect or not.

When we used 1 ML of SrO as a buffer layer, the silicon was sufficiently passivated against oxidation at $P(O_2)$ ∼ 2.5 × 10^{-8} Torr and T_{Sub} ≲ 280 °C that EuO could be grown epitaxially on silicon at about the same deposition conditions as on YAlO$_3$. This is corroborated by STEM-EELS measurements of a EuO-film deposited on a 1-ML-thick SrO buffer layer at T_{Sub} = 200 °C using the optimized deposition conditions (see the Supplemental Material [35]). In these measurements we find no indications of europium silicides, europium valence changes, or interdiffusion. At T_{Sub} ≳ 280 °C, extra diffraction spots appeared in RHEED as soon as the EuO-deposition started, which could be a sign of the breakdown of the buffer layer and the formation of europium silicides.

Our findings show that a single ML of SrO can be sufficient to suppress interdiffusion and unwanted reactions at the interface if the deposition temperature is chosen to be low enough and $P(O_2)$ adjusted within a narrow growth window. Because of the insulating nature of SrO (band gap of ∼5.3 eV at 80 K [36]), the introduction of 1 ML of SrO is, however, expected to lead to a tunnel contact between EuO and silicon, also blocking ohmic spin injection.

For reducing the influence of the buffer layer on the electrical properties of the EuO/SrO/Si interface we therefore tried to minimize the amount of SrO. To investigate the possibility of conductance matching the EuO to the substrate we also started doping the EuO with lanthanum. These experiments showed that lanthanum doping up to 1% does not considerably change the growth behavior of Eu$_{1-x}$La$_x$O on silicon. Furthermore, we found that a minimum of $\frac{1}{2}$ ML of SrO was required to ensure good epitaxy of Eu$_{1-x}$La$_x$O on silicon. We performed no STEM-EELS measurements on samples with coverages between zero and $\frac{1}{2}$ ML, because *in situ* RHEED imaging indicated a bad interface with the formation of unwanted phases, similar to the case when no SrO buffer was used.

The maximum deposition temperature for Eu$_{1-x}$La$_x$O on SrO buffer layers of $\frac{1}{2}$ ML thickness is also around T_{Sub} = 280 °C. At higher temperatures extra spots appear in RHEED
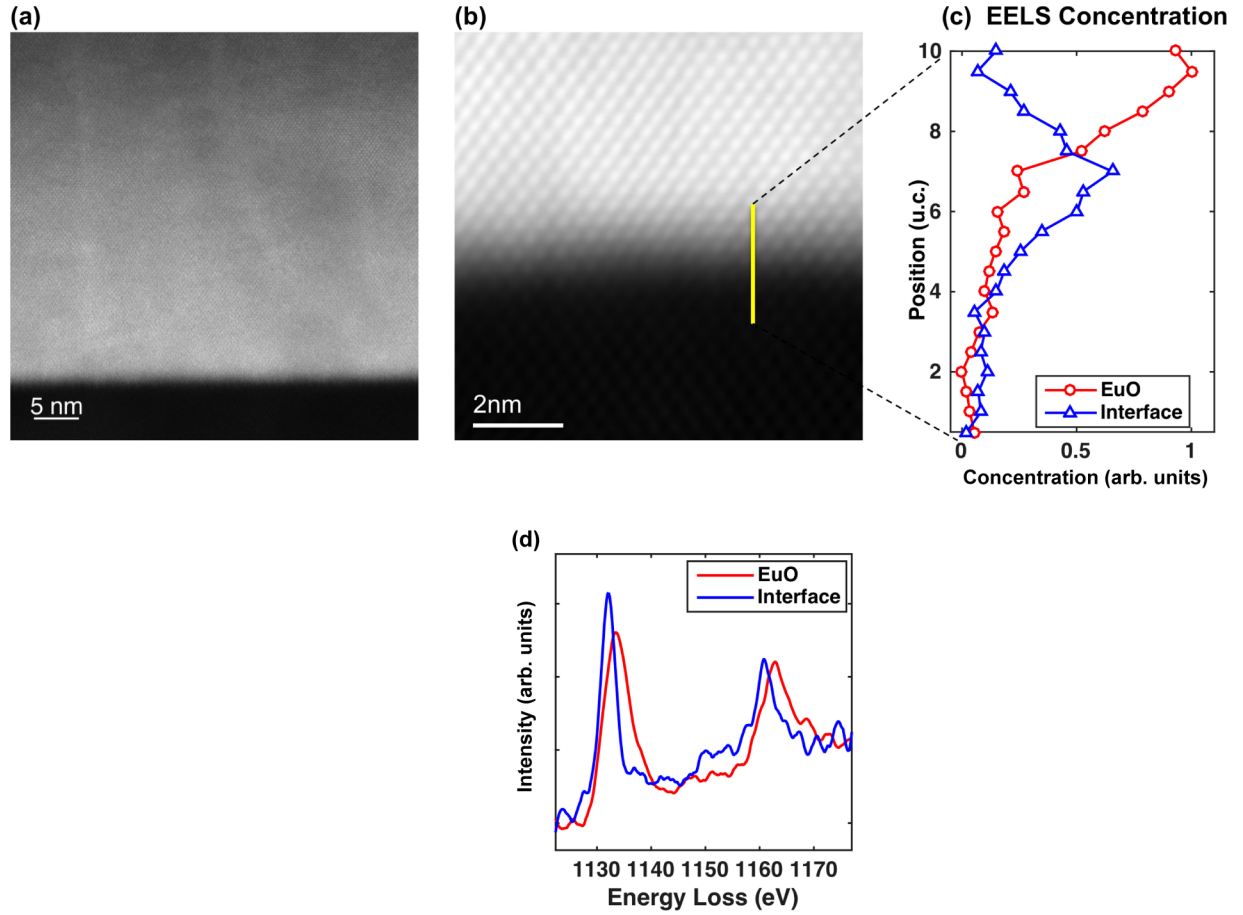
FIG. 1. STEM-EELS measurements of a 0.1% La-doped EuO film with a $\frac{1}{2}$ ML SrO buffer on silicon. Low-magnification and high-magnification HAADF-STEM images of the interface are shown in (a) and (b), respectively. The interface is abrupt and free of impurity layers. (c) An EELS concentration profile across the interface shows a region near the interface with a slightly different valence. (d) The EELS spectra from the Eu-$M_{4,5}$ edge showing the two distinct spectra—one from the EuO film and the other from the interfacial region.

directly after starting the $Eu_{1-x}La_xO$-deposition, indicating the formation of impurity phases.

We use scanning transmission electron microscopy (STEM) in conjunction with electron energy loss spectroscopy (EELS) to investigate the structure and bonding at the EuO/Si interface. Samples were prepared as in Ref. [25] to minimize exposure to air during the preparation process. The Sr was not detectable in the STEM-EELS measurements (see the Supplemental Material for further details).

STEM-EELS analysis of a 0.1% La-doped EuO film with a $\frac{1}{2}$ ML SrO buffer grown at $T_{Sub} = 250\,^\circ C$ is shown in Fig. 1. As shown in Fig. 1(a), and in higher resolution in Fig. 1(b), the interface is free of impurity layers and does not show any detectable signs of interdiffusion. Interestingly, the amount of disorder we observe at the interface is much less pronounced than for the case of the sample grown at $T_{Sub} = 200\,^\circ C$. We collected EELS spectra from the Eu-$M_{4,5}$ edge across the interface to look for chemical changes in the interfacial layers. As shown in Fig. 1(c), we observe a slight reduction in the valence localized to a narrow region of 1–2 unit cells (u.c.) near the interface [the spectra are shown in Fig. 1(d)]. We are not sure what causes this effect. We can exclude the formation of a significant amount of europium silicides, as these silicides reveal themselves in our STEM measurements as bright spots

(see the Supplemental Material, part 1 of Fig. S6). Overoxidation of europium oxide would lead to an increase in the valence, not a reduction.

It is also very unlikely that europium metal could exist just at the interface, because of the high reactivity of europium atoms with oxygen and silicon. We also find no indications of europium metal clusters at the interface, which should be clearly visible in STEM. In addition, the EELS spectra of the EuO and the interface look very similar, except for the small shift. The slight reduction in the europium valence at the interface therefore might be an effect related to interface defects or it may be characteristic for the clean EuO/SrO/Si interface. Further studies would be needed to clarify this question, possibly taking into account the atomic reconstruction of this interface and lanthanum doping.

We infer that the higher growth temperature of $T_{Sub} = 250\,^\circ C$ allows improved crystallization of the film after strain relaxation due to the 5.6% lattice mismatch between EuO and silicon, while still avoiding strong interdiffusion and unwanted interface reactions. This is corroborated by the reduced full width at half maximum of the EuO 002 rocking curve of the film grown at the higher temperature [Fig. 2(a)]. In θ-2θ scans we find no indications of impurity phases in either sample [Fig. 2(b)].
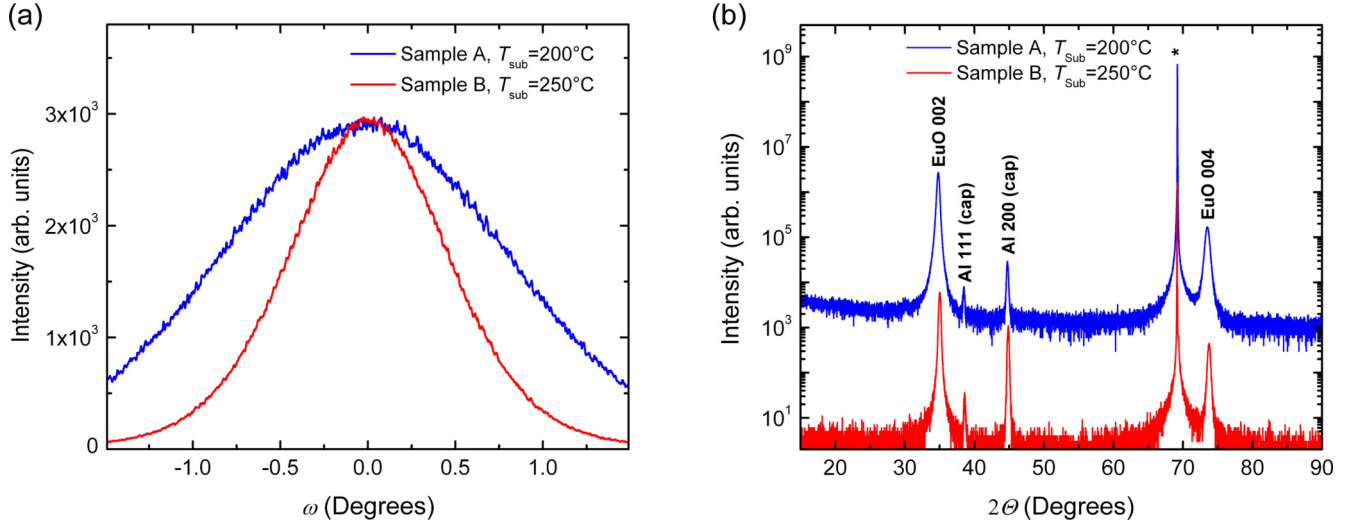
FIG. 2. X-ray diffraction scans of samples A (undoped EuO, 1 ML SrO) and B (0.1% La-doped EuO, $\frac{1}{2}$ ML SrO) deposited at $T_{Sub} = 200\,°C$ and $250\,°C$, respectively. (a) Rocking curves of the samples demonstrating that increasing the substrate temperature considerably improves the crystalline quality of the film. (b) θ-2θ scans of the same samples showing no indications of unwanted phases. Asterisks (*) denote substrate peaks; the aluminum peaks result from the polycrystalline aluminum capping layer.

In the STEM image [Fig. 1(b)], we also see that there is a ~1-nm-thick layer at the EuO/SrO/Si interface where individual europium atoms are still visible, but not as clearly as in the bulk EuO. This indicates some disorder at the interface, which is also consistent with the change in the RHEED patterns observed during the initial stages of film growth (Fig. 3). After deposition of strontium and oxidation of strontium to SrO, the surface still shows sharp and very bright RHEED streaks indicating a well-ordered and flat surface [Fig. 3(a)]. During the deposition of the first monolayers of EuO the RHEED diffraction maxima dim and the background signal increases, indicating a reduction in the structural perfection of the growing film compared to the substrate. In this stage dim streaks develop at the original substrate diffraction maxima positions indicating lattice-matched growth of EuO on silicon [Fig. 3(b)]. During the deposition of EuO from ML 1 through MLs 2–3, these RHEED streaks become sharper and the background decreases [Fig. 3(c)]. After 2–3 MLs of EuO, transitional faint extra spots and ringlike structures

appear and the streaks shift toward larger angles, consistent with the structural disorder resulting from the relaxation of EuO towards its bulk lattice parameter of 5.141 Å beyond this critical film thickness [Fig. 3(d)]. Due to the large lattice mismatch between EuO and silicon of +5.6%, the relaxation of EuO grown on silicon is expected. From the evolution of our RHEED patterns we conclude that the critical thickness for the onset of relaxation of EuO on SrO-buffered silicon is 2–3 MLs at a substrate temperature of $250\,°C$. As the EuO deposition continues, the extra spots vanish after a few nanometers, the streaks became sharper, and the background decreases indicating improving crystallinity of the EuO [Figs. 3(e) and 3(f)].

The magnetic properties of the samples were measured by SQUID magnetometry (Fig. 4). The Curie temperature of sample B, which is doped with 0.1% of lanthanum, is increased to 78 K, as expected from this amount of lanthanum doping [14]. The saturation magnetization of the same sample is $6.8 \pm 0.2 \, \mu B/Eu$, which is consistent with the theoretical maximum of $7 \, \mu_B/Eu$ and measurement of bulk EuO [37].
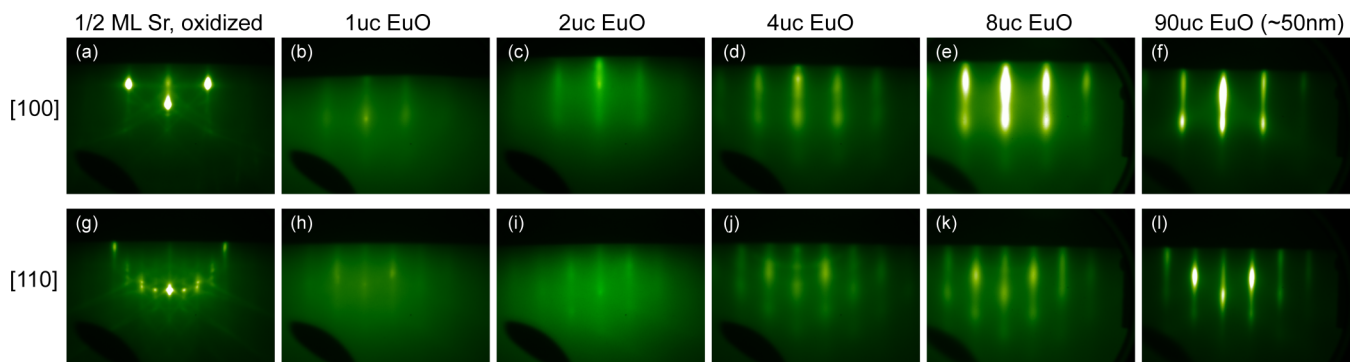

FIG. 3. RHEED images from various stages of epitaxy of EuO on silicon at a substrate temperature of $T_{Sub} = 250\,°C$. (a)/(g) Protection of the silicon substrates against unwanted interface reactions with $\frac{1}{2}$ ML of SrO prior to the EuO deposition. Panels (b)–(f) and (h)–(l): Images taken at increasing thickness of the growing EuO film, given in unit cells (uc, where 1 uc = 2 MLs). The photographs were recorded with the incident beam azimuths pointing along the [100] [see (a)–(h)] and [110] [see (g)–(l)] directions of the EuO film (and silicon substrate).
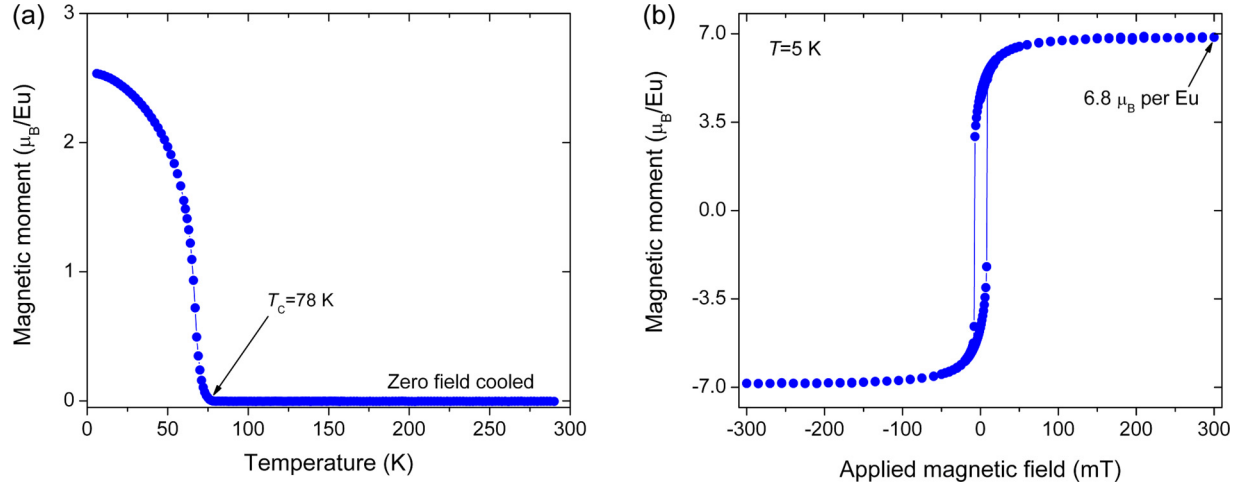
FIG. 4. (a) Temperature dependence of the in-plane magnetization of a 50-nm-thick $Eu_{0.999}La_{0.001}O$ film grown on a 001-oriented silicon substrate at $T_{Sub} = 250\,°C$ using $\frac{1}{2}$ ML of SrO as a buffer layer (sample B). The Curie temperature determined from this measurement is 78 K. (b) Hysteresis loop of the same sample showing a saturation magnetization of 6.8 μ_B/Eu atom of the film.

Because of the large magnetic moment of the europium atoms and the relatively small amount of disorder found at the $Eu_{1−x}La_xO/SrO/Si$ interface we expect electrical currents in the $Eu_{1−x}La_xO$ to be spinpolarized close to the interface at temperatures $T < 78$ K.

IV. CONCLUSIONS

At the high-quality $Eu_{1−x}La_xO/\frac{1}{2}$ML SrO/Si interfaces produced in this study we expect approximately every other europium atom from the $Eu_{1−x}La_xO$ to be directly bonded to a silicon atom. Reducing the amount of SrO at the interface to half a monolayer and avoiding interface impurities may possibly avoid the formation of a tunnel contact between the materials. In addition, avoiding europium valence changes allows the strong magnetism of the $Eu_{1−x}La_xO$ to be maintained at the interface. It is conceivable that such a structure will enable the high spin polarization of electrical currents to propagate across the interface and ultimately allow direct ohmic injection of spin-polarized currents from the conductance-matched $Eu_{1−x}La_xO$ into the silicon substrate. Successful spin injection from the $Eu_{1−x}La_xO$ into the silicon also depends on the band structures of the materials at the interface. The band gaps of EuO (1.12 eV [38]) and Si (1.1 eV) match almost precisely. In a naïve picture this should be ideal for spin injection. Recently, Lev *et al.* used soft-x-ray ARPES to investigate the band structure of EuO thin films (1.3 nm) deposited directly onto silicon [29]. They estimated the conduction band offset to be 1.0 eV, which adds to the technological potential of the Si/EuO system for spintronic devices.

The details of the interface band structure and spin injection efficiency, however, also depend on the precise atomic structure of the interface, including possible shifts in atomic positions and associated dipole formation, the presence and distribution of europium silicides, europium and silicon oxides, and the atomic species used for surface protection. Measurements employing STEM-EELS and density func-

tional theory calculations based on an atomistic model of the various interface structures could be highly beneficial to determine the best interface candidates for efficient spin injection, which may ultimately result in highly efficient $Eu_{1−x}La_xO/Si$ spin filter contacts.

In summary, we have optimized the epitaxial growth of undoped and La-doped EuO on silicon. We found that by using relatively low substrate temperatures (200–250 °C) and employing very accurate control of the oxygen partial pressure it is possible to deposit epitaxial $Eu_{1−x}La_xO$ on SrO-buffered silicon with no detectable impurity phases as confirmed by atomically resolved STEM-EELS measurements, which have demonstrated the ability of detecting even very small amounts of impurity phases. The minimum amount of SrO required for avoiding the formation of reaction phases at the interface was $\frac{1}{2}$ monolayer and the sweet-spot substrate temperature that yielded the best atomic interface structure was $T_{Sub} = 250\,°C$. At just a little bit higher substrate temperatures around $T_{Sub} = 280\,°C$ the buffer layer no longer avoided unwanted interface reactions. The growth technique developed therefore provides a promising alternative starting point for performing spin-injection studies in the $Eu_{1−x}La_xO/SrO/Si$ system.

[1] G. Schmidt, D. Ferrand, L. W. Molenkamp, A. T. Filip, and B. J. van Wees, Phys. Rev. B **62**, R4790 (2000).

[2] C. L. Dennis, C. Sirisathitkul, G. J. Ensell, J. F. Gregg, and S. M. Thompson, J. Phys. D: Appl. Phys. **36**, 81 (2003).

[3] B. T. Jonker, G. Kioseoglou, A. T. Hanbicki, C. H. Li, and P. E. Thompson, Nat. Phys. **3**, 542 (2007).

[4] I. Appelbaum, B. Huang, and D. J. Monsma, Nature (London) **447**, 295 (2007).

[5] K. D. Belashchenko, J. K. Glasbrenner, and A. L. Wysocki, Phys. Rev. B **86**, 224402 (2012).

[6] A. Schmehl, V. Vaithyanathan, A. Herrnberger, S. Thiel, C. Richter, M. Liberati, T. Heeg, M. Röckerath, L. Fitting Kourkoutis, S. Mühlbauer, P. Böni, D. A. Muller, Y. Barash, J. Schubert, Y. Idzerda, J. Mannhart, and D. G. Schlom, Nat. Mater. **6**, 882 (2007).

[7] A. Melville, T. Heeg, T. Mairoser, A. Schmehl, D. Shai, E. Monkman, J. Harter, B. Hollaender, J. Schubert, K. M. Shen, J. Mannhart, and D. G. Schlom, Appl. Phys. Lett. **100**, 222101 (2012).

[8] A. G. Swartz, J. Ciraldo, J. J. I. Wong, Y. Li, W. Han, T. Lin, S. Mack, J. Shi, D. D. Awschalom, and R. K. Kawakami, Appl. Phys. Lett. **97**, 112509 (2010).

[9] P. G. Steeneken, L. H. Tjeng, I. Elfimov, G. A. Sawatzky, G. Ghiringhelli, N. B. Brookes, and D.-J. Huang, Phys. Rev. Lett. **88**, 047201 (2002).

[10] M. W. Shafer and T. R. McGuire, J. Appl. Phys. **39**, 588 (1968).

[11] T. Mairoser, A. Schmehl, A. Melville, T. Heeg, L. Canella, P. Böni, W. Zander, J. Schubert, D. E. Shai, E. J. Monkman, K. M. Shen, D. G. Schlom, and J. Mannhart, Phys. Rev. Lett. **105**, 257206 (2010).

[12] H. Miyazaki, H. J. Im, K. Terashima, S. Yagi, M. Kato, K. Soda, T. Ito, and S. Kimura, Appl. Phys. Lett. **96**, 232503 (2010).

[13] T. Mairoser, F. Loder, A. Melville, D. G. Schlom, and A. Schmehl, Phys. Rev. B **87**, 014416 (2013).

[14] R. Held, T. Mairoser, A. Melville, J. A. Mundy, M. E. Holtz, D. Hodash, Z. Wang, J. T. Heron, S. T. Dacek, B. Holländer, D. A. Muller, and D. G. Schlom, Phys. Rev. Mater. **4**, 104412 (2020).

[15] T. R. McGuire and M. W. Shafer, J. Appl. Phys. **35**, 984 (1964).

[16] F. Holtzberg, T. R. McGuire, S. Methfessel, and J. C. Suits, Phys. Rev. Lett. **13**, 18 (1964).

[17] K. Y. Ahn and T. R. McGuire, J. Appl. Phys. **39**, 5061 (1968).

[18] K. Y. Ahn and M. W. Shafer, J. Appl. Phys. **41**, 1260 (1970).

[19] A. Mauger, M. Escorne, C. Godart, J. P. Desfours, and J. C. Achard, J. Phys. Colloq. **41**, C5-263 (1980).

[20] S. G. Altendorf, A. Reisner, C.-F. Chang, N. Hollmann, D. Rata, and L. H. Tjeng, Appl. Phys. Lett. **104**, 052403 (2014).

[21] N. J. C. Ingle and I. S. Elfimov, Phys. Rev. B **77**, 121202(R) (2008).

[22] S. G. Altendorf, N. Hollmann, R. Sutarto, C. Caspers, R. C. Wicks, Y.-Y. Chin, Z. Hu, H. Kierspel, I. S. Elfimov, H. H.

Hsieh, H.-J. Lin, C. T. Chen, and L. H. Tjeng, Phys. Rev. B **85**, 081201(R) (2012).

[23] J. Lettieri, V. Vaithyanathan, S. K. Eah, J. Stephens, V. Sih, D. D. Awschalom, J. Levy, and D. G. Schlom, Appl. Phys. Lett. **83**, 975 (2003).

[24] C. Caspers, M. Müller, A. X. Gray, A. M. Kaiser, A. Gloskovskii, C. S. Fadley, W. Drube, and C. M. Schneider, Phys. Rev. B **84**, 205217 (2011).

[25] J. A. Mundy, D. Hodash, A. Melville, R. Held, T. Mairoser, D. A. Muller, L. F. Kourkoutis, A. Schmehl, and D. G. Schlom, Appl. Phys. Lett. **104**, 091601 (2014).

[26] D. V. Averyanov, Y. G. Sadofyev, A. M. Tokmachev, A. E. Primenko, I. A. Likhachev, and V. G. Storchak, ACS Appl. Mater. Interfaces **7**, 6146 (2015).

[27] D. V. Averyanov, C. G. Karateeva, I. A. Karateev, A. M. Tokmachev, A. L. Vasiliev, S. I. Zolotarev, I. A. Likhachev, and V. G. Storchak, Sci. Rep. **6**, 22841 (2016).

[28] C. Caspers, A. Gloskovskii, M. Gorgoi, C. Besson, M. Luysberg, K. Z. Rushchanskii, M. Ležaić, C. S. Fadley, W. Drube, and M. Müller, Sci. Rep. **6**, 22912 (2016).

[29] L. L. Lev, D. V. Averyanov, A. M. Tokmachev, F. Bisti, V. A. Rogalev, V. N. Strocov, and V. G. Storchak, J. Mater. Chem. C **5**, 192 (2017).

[30] D. V. Averyanov, I. S. Sokolov, A. M. Tokmachev, I. A. Karateev, O. A. Kondratev, A. N. Taldenkov, O. E. Parfenov, and V. G. Storchak, J. Magn. Magn. Mater. **459**, 136 (2018).

[31] D. V. Averyanov, I. S. Sokolov, I. A. Karateev, A. N. Taldenkov, O. E. Parfenov, A. M. Tokmachev, and V. G. Storchak, Adv. Funct. Mater. **31**, 2010269 (2021).

[32] R. Farshchi and M. Ramsteiner, J. Appl. Phys. **113**, 191101 (2013).

[33] R. W. Ulbricht, A. Schmehl, T. Heeg, J. Schubert, and D. G. Schlom, Appl. Phys. Lett. **93**, 102105 (2008).

[34] R. Sutarto, S. G. Altendorf, B. Coloru, M. Moretti Sala, T. Haupricht, C. F. Chang, Z. Hu, C. Schüßler-Langeheine, N. Hollmann, H. Kierspel, J. A. Mydosh, H. H. Hsieh, H.-J. Lin, C. T. Chen, and L. H. Tjeng, Phys. Rev. B **80**, 085308 (2009).

[35] See Supplemental Material at http://link.aps.org/supplemental/10.1103/PhysRevMaterials.5.124419 for further details on the development of the low-temperature deposition method of $Eu_{1-x}La_xO$ films and for additional STEM-EELS data.

[36] A. S. Rao and R. J. Kearney, Phys. Status Solidi B **95**, 243 (1979).

[37] B. T. Matthias, R. M. Bozorth, and J. H. Van Vleck, Phys. Rev. Lett. **7**, 160 (1961).

[38] *Numerical Data and Functional Relationships in Science and Technology*, Landolt-Börnstein New Series, Group III, Vol. 17, edited by K.-H. Hellwege and O. Madelung (Springer, Berlin, 1984), p. 321.